

Tetrasaccharide Resin Glycosides with Nitric Oxide Production Inhibitory Activity from *Cuscuta campestris*

Jae Sang Han, Jun Gu Kim, Yong Beom Cho, Joon Su Jang, Vu Quan Dang, Dongho Lee, Mi Kyong Lee, Jin Woo Lee, and Bang Yeon Hwang*



Cite This: *J. Nat. Prod.* 2025, 88, 2117–2126



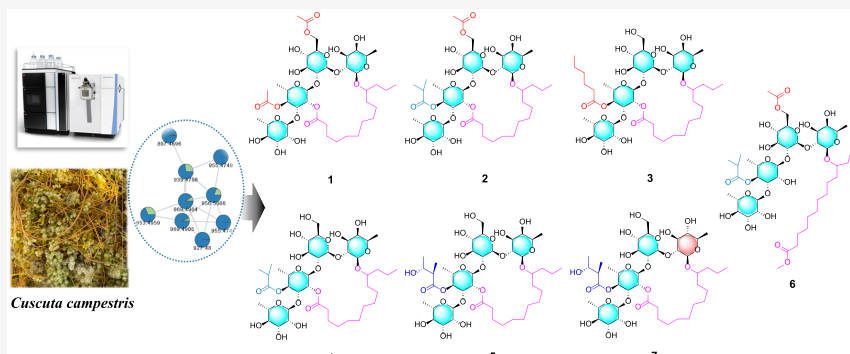
Read Online

ACCESS |

Metrics & More

Article Recommendations

Supporting Information



ABSTRACT: LC-HRMS/MS-based molecular-network-guided chemical investigation of *Cuscuta campestris* led to the isolation of seven undescribed tetrasaccharide-type resin glycosides (**1–7**). Their structures were elucidated using 1D and 2D NMR and HRESIMS analysis. Isolated resin glycosides were comprised of D-glucose, D-fucose, D-quinovose, and L-rhamnose, and these monosaccharides were partially acylated with acetyl, isobutyryl, n-hexanoyl, and niloyl organic acids. The absolute configuration of aglycones were determined as S-configuration using Mosher's method after acid hydrolysis of resin glycoside fraction. All compounds were evaluated for their inhibitory activity against the production of nitric oxide in RAW 264.7 cells. Compounds **2** and **3** exhibited inhibitory activity, with IC₅₀ values of 14.3 and 10.4 μM, respectively.

Cuscuta campestris Yunck. (Convolvulaceae) is a holoparasitic annual plant native to North America and widely distributed across the globe. This species is characterized by a degenerated root system and leaves reduced to minute, alternate scales, and it exhibits low host specificity, enabling it to parasitize a diverse range of plant species.¹ Despite the biological significance of genus *Cuscuta*,² comprehensive phytochemical and bioactivity investigations of *C. campestris* remain scarce. Ethnopharmacological studies, along with a limited number of bioactivity assessments, have highlighted its anti-inflammatory^{3,4} and hepatoprotective⁵ properties. However, phytochemical analyses conducted to date have only led to the isolation and identification of flavonoids, lignans, caffeic acid derivatives, and triterpenoids.^{5–7}

The family Convolvulaceae is well-known for its production of structurally diverse resin glycosides,^{8,9} which are among the most characteristic metabolites of this family. These compounds are composed of mono- to heptasaccharides acylated with various C₁₀ to C₁₈ fatty acids, and their dimeric forms have also been identified. Resin glycosides have been reported to exhibit a broad spectrum of bioactivities, including the reversal of multidrug resistance in bacterial pathogens and human cancer

cells,^{10,11} as well as anti-inflammatory, cytotoxic,¹² antidiabetic,¹³ antiviral,^{14,15} and neuroprotective properties.¹⁶

To investigate the identification of bioactive resin glycosides in *C. campestris*, LC-MS-based molecular networking (MN)¹⁷ and bioactivity evaluation were employed. In the network, a cluster of resin glycoside nodes was identified through spectral library matching and the Node Annotation Propagation (NAP) tool.¹⁸ Based on the MN results, nonchromophoric resin glycosides were confirmed to be distributed in the ethyl acetate (EtOAc)-soluble fraction, which exhibited the highest inhibitory activity against nitric oxide (NO) production in LPS-induced RAW 264.7 cells among the solvent fractions. Utilizing the node information from the MN, these compounds were successfully tracked and isolated.

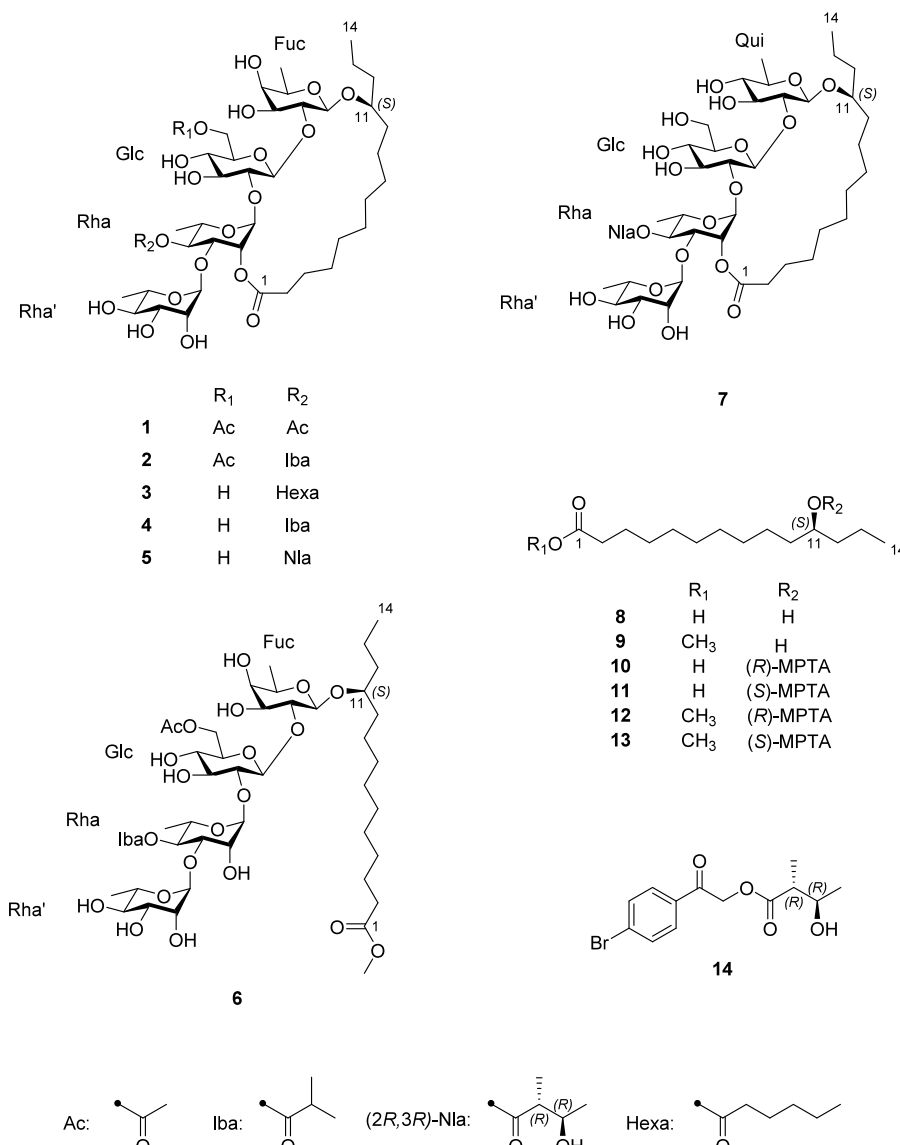
Received: June 12, 2025

Revised: August 25, 2025

Accepted: August 28, 2025

Published: September 9, 2025





As a result of isolation guided by MN and bioactivity evaluation, a total of seven previously undescribed resin glycosides, named campestridins A–G, were isolated from *C. campestris*. Their structures were elucidated using 1D and 2D NMR spectroscopy and HRESIMS, and the absolute configurations of monosaccharides, aglycones, and nilic acid were determined following acidic or alkaline hydrolysis of the resin glycoside fraction. Furthermore, the inhibitory effects of all isolated compounds on the NO production in RAW 264.7 macrophages were evaluated.

RESULTS AND DISCUSSION

In the LC-MS molecular networking analysis of *n*-hexane, CH₂Cl₂, and EtOAc-soluble fractions, the GNPS spectral library search and NAP tool results predicted that the nodes in cluster 1 with *m/z* values ranging from 800 to 1000 corresponded to resin glycosides. However, none of the nodes matched any existing library. To further support this prediction, positive-ion HRESIMS tandem mass analysis was conducted on node 1 (Figure S2), for which the molecular formula was determined as C₄₄H₇₄O₂₁ based on the *m/z* value of 939.480. The following fragment ions were identified: *m/z* 793.422 [C₃₈H₆₅O₁₇⁺, (939.480–C₆H₁₀O₄)⁺], 647.364 [C₃₂H₅₅O₁₃⁺, (793.422–C₆H₁₀O₄)⁺],

C₆H₁₀O₄)⁺], 589.358 [C₃₀H₅₃O₁₁⁺, (793.422–C₈H₁₂O₆)⁺], 443.300 [C₂₄H₄₃O₇⁺, (589.358–C₆H₁₀O₄)⁺], and 337.236 [C₂₀H₃₃O₄⁺, (425.289–C₄H₈O₂)⁺]. These fragment ions are consistent with the structural characteristics of resin glycosides, which are composed of hexo- and deoxyhexose units. These resin glycosides, mainly distributed in the EtOAc-soluble fraction, were targeted and isolated based on the chromatographic information in MN, leading to the efficient isolation of seven previously undescribed tetrasaccharide resin glycosides (**1**–**7**).

Compound **1** was obtained as a white amorphous powder, and its HRESIMS data (*m/z* 911.4483 [M + H]⁺, calcd. 911.4482) established its molecular formula as C₄₂H₇₀O₂₁. Analysis of the 1D NMR and HSQC data revealed four anomeric protons [δ_H 4.71 (Fuc H-1, d, *J* = 7.8 Hz), 5.76 (Glc H-1, d, *J* = 7.8 Hz), 5.68 (Rha H-1, br s), 5.40 (Rha' H-1, br s)], two acetyl groups [δ_H 1.82 (Ac H-2, s), 1.92 (Ac' H-2, s)], as well as one methyl group [δ_H 0.88 (Agly H-14, t, *J* = 6.7 Hz)] and oxygenated methine protons [δ_H 3.86 (Agly H-11, m)] of a tetradecanoyl moiety (Tables 1 and 2). The HRESIMS and NMR data indicated that compound **1** is a resin glycoside composed of four hexose units, two acetyl groups, and a tetradecanoyl group. In the COSY data, the proton spin systems of each monosaccharide were traced

Table 1. ^1H NMR Spectroscopic Data for Compounds 1–4 in Pyridine- d_5

	1 ^a	2 ^b	3 ^c	4 ^c
Position	δ_{H} (J in Hz)	δ_{H} (J in Hz)	δ_{H} (J in Hz)	δ_{H} (J in Hz)
Fuc-1	4.71, d (7.8)	4.71, d (7.8)	4.71, d (7.8)	4.74, d (7.8)
2	4.71, m	4.71, m	4.78, dd (7.8, 9.2) 8.8)	4.78, dd (7.8, 8.8)
3	4.21, m	4.21, m	4.22, m	4.22, dd (1.9, 8.8)
4	3.94, br s	3.99, br s	3.97, br s	4.00, br s
5	3.78, q (6.4)	3.81, q (6.3)	3.82, q (6.3)	3.82, q (6.3)
6	1.53, d (6.4)	1.54, d (6.3)	1.57, d (6.3)	1.56, d (6.3)
Glc-1	5.76, d (7.8)	5.76, d (7.8)	5.82, d (7.8)	5.81, d (7.7)
2	3.90, dd (7.8, 8.8)	3.91, dd (7.8, 8.9)	3.94, dd (7.8, 8.9)	3.93, dd (7.7, 8.6)
3	4.08, br t (8.8)	4.09, br t (8.9)	4.11, br t (8.9)	4.11, dd (8.6, 8.9)
4	3.95, m	3.95, m	4.09, m	4.09, m
5	3.62, m	3.61, m	3.55, m	3.56, dt (4.1, 9.1)
6a	4.52, m	4.55, m	4.06, m	4.09, m
6b	4.56, m	4.55, m	4.09, m	4.09, m
Rha-1	5.68, br s	5.70, br s	5.72, br s	5.72, br s
2	6.16, br s	6.16, br s	6.17, br s	6.16, br s
3	4.65, dd (3.3, 9.9)	4.71, m	4.71, dd (3.3, 9.8)	4.71, dd (3.3, 9.9)
4	5.70, t (9.9)	5.70, t (9.9)	5.74, t (9.8)	5.70, t (9.9)
5	4.89, dq (6.2, 9.9)	4.91, dq (6.2, 9.9)	4.95, m	4.93, dq (6.2, 9.9)
6	1.65, d (6.2)	1.62, d (6.2)	1.67, d (6.2)	1.62, d (6.2)
Rha'-1	5.40, br s	5.39, br s	5.43, br s	5.39, br s
2	4.49, br s	4.48, br s	4.51, br s	4.48, br s
3	4.52, m	4.50, m	4.51, m	4.49, m
4	4.25, br t (9.1)	4.25, br t (9.2)	4.25, br t (9.3)	4.25, dd (9.0, 9.4)
5	4.37, dq (6.3, 9.1)	4.37, dq (6.3, 9.2)	4.38, dq (9.3, 6.2)	4.37, dq (6.3, 9.4)
6	1.62, d (6.3)	1.63, d (6.3)	1.62, d (6.2)	1.62, d (6.3)
Agly-2a	2.22, ddd (3.6, 9.2, 14.0)	2.22, ddd (3.6, 8.8, 13.6)	2.21, ddd (3.6, 9.3, 13.5)	2.21, ddd (3.6, 9.3, 13.5)
2b	2.31, ddd (3.6, 8.1, 14.0)	2.30, ddd (3.6, 7.6, 13.6)	2.30, m	2.30, ddd (3.6, 8.3, 13.5)
3a	1.50, m	1.50, m	1.49, m	1.50, m
3b	1.62, m	1.61, m	1.62, m	1.61, m
4a	1.26, m	1.28, m	1.26, m	1.26, m
4b	1.40, m	1.40, m	1.40, m	1.39, m
11	3.86, m	3.88, m	3.89, m	3.89, m
12a	1.52, m	1.52, m	1.51, m	1.52, m
12b	1.72, m	1.72, m	1.71, m	1.72, m
13	1.50, m	1.51, m	1.49, m	1.50, m
14	0.88, t (6.7)	0.89, t (6.9)	0.86, t (7.0)	0.86, t (7.0)
Ac-2	1.82, s	1.82, s	-	-
Ac'-2	1.92, s	-	-	-
Iba-2	-	2.50, h (7.0)	-	2.51, h (7.0)
3	-	1.11, d (7.0)	-	1.12, d (7.0)
4	-	1.11, d (7.0)	-	1.11, d (7.0)
Hexa-2	-	-	2.27, m	-
3	-	-	1.60, m	-
4	-	-	1.16, m	-
5	-	-	1.16, m	-
6	-	-	0.77, t (7.0)	-

^aRecorded at 900 MHz. ^bRecorded at 400 MHz.**Table 2.** ^{13}C NMR Spectroscopic Data for Compounds 1–4 in Pyridine- d_5

	1 ^a	2 ^b	3 ^c	4 ^c
Position	δ_{C} , type	δ_{C} , type	δ_{C} , type	δ_{C} , type
Fuc-1	102.0, CH	101.9, CH	102.2, CH	102.2, CH
2	75.0, CH	75.2, CH	74.7, CH	74.9, CH
3	76.7, CH	76.8, CH	76.7, CH	76.7, CH
4	73.4, CH	73.5, CH	73.4, CH	73.4, CH
5	71.2, CH	71.2, CH	71.3, CH	71.3, CH
6	17.3, CH ₃	17.3, CH ₃	17.3, CH ₃	17.3, CH ₃
Glc-1	100.8, CH	100.9, CH	100.6, CH	100.7, CH
2	85.1, CH	84.9, CH	85.1, CH	85.0, CH
3	77.6, CH	77.6, CH	77.8, CH	77.8, CH
4	71.8, CH	71.8, CH	72.3, CH	72.3, CH
5	74.4, CH	74.5, CH	77.0, CH	77.0, CH
6	64.3, CH ₂	64.3, CH ₂	62.5, CH ₂	62.5, CH ₂
Rha-1	100.4, CH	100.2, CH	100.2, CH	100.2, CH
2	72.8, CH	72.8, CH	72.8, CH	72.8, CH
3	76.5, CH	76.4, CH	76.5, CH	76.4, CH
4	73.9, CH	73.5, CH	73.7, CH	73.6, CH
5	66.8, CH	66.9, CH	66.9, CH	66.9, CH
6	18.7, CH ₃	18.8, CH ₃	18.9, CH ₃	18.8, CH ₃
Rha'-1	104.0, CH	104.0, CH	104.0, CH	104.0, CH
2	72.7, CH	72.5, CH	72.6, CH	72.5, CH
3	72.6, CH	72.6, CH	72.6, CH	72.6, CH
4	73.8, CH	73.8, CH	73.9, CH	73.8, CH
5	70.8, CH	70.7, CH	70.7, CH	70.7, CH
6	18.6, CH ₃	18.6, CH ₃	18.6, CH ₃	18.6, CH ₃
Agly-1	173.2, C	173.2, C	173.2, C	173.2, C
2	35.0, CH ²	34.9, CH ₂	35.0, CH ₂	34.9, CH ₂
3	26.0, CH ²	26.0, CH ₂	26.1, CH ₂	26.0, CH ₂
4	28.3, CH ²	28.3, CH ₂	28.3, CH ₂	28.3, CH ₂
11	78.6, CH	78.6, CH	78.9, CH	78.9, CH
12	37.9, CH ²	37.9, CH ₂	37.9, CH ₂	37.9, CH ₂
13	19.1, CH ²	19.2, CH ₂	19.2, CH ₂	19.1, CH ₂
14	14.4, CH ₃	14.4, CH ₃	14.4, CH ₃	14.4, CH ₃
Ac-1	170.8, C	170.8, C	-	-
2	20.6, CH ₃	20.6, CH ₃	-	-
Ac'-1	170.4, C	-	-	-
2	20.7, CH ₃	-	-	-
Iba-1	-	176.3, C	-	176.4, C
2	-	34.4, CH	-	34.4, CH
3	-	19.1, CH ₃	-	19.2, CH ₃
4	-	19.1, CH ₃	-	19.2, CH ₃
Hexa-1	-	-	173.2, C	-
2	-	-	34.5, CH ₂	-
3	-	-	25.1, CH ₂	-
4	-	-	31.4, CH ₂	-
5	-	-	22.5, CH ₂	-
6	-	-	14.0, CH ₃	-

^aRecorded at 225 MHz. ^bRecorded at 100 MHz.

correlation from Fuc H-1 (δ_{H} 4.71) to Agly C-11 (δ_{C} 78.6), along with the COSY correlations of H₃-14/H₂-13/H₂-12/H₁-11 and HMBC correlations shown in Figure 1. The sugar connectivity was determined through HMBC correlations (Figures 1 and S8) from Glc H-1 (δ_{H} 5.76) to Fuc C-2 (δ_{C} 75.0), from Rha H-1 (δ_{H} 5.68) to Glc C-2 (δ_{C} 85.1), and from Rha' H-1 (δ_{H} 5.40) to Rha C-3 (δ_{C} 76.5). The HMBC correlations of Glc H-6 (δ_{H} 4.52) with Ac C-1 (δ_{C} 170.8) and Rha H-4 (δ_{H} 5.70) with Ac' C-1 (δ_{C} 170.4) established the positions of the acetyl groups. Additionally, the linkage of the

based on their respective anomeric protons. The aglycone was identified as 11-hydroxytetradecanoic acid based on the HMBC

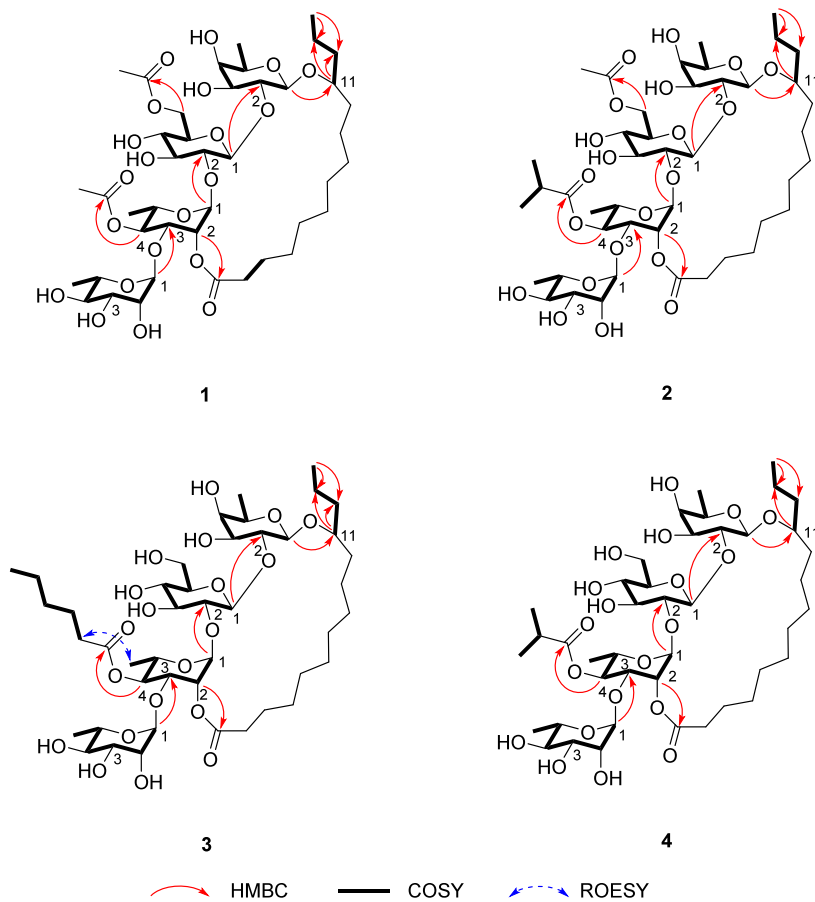


Figure 1. Key HMBC and COSY correlations of compounds 1–4.

aglycone was confirmed by HMBC correlations from Rha H-2 (δ_H 6.16) to Agly C-1 (δ_C 173.2) and from Fuc H-1 (δ_H 4.71) to Agly C-11 (δ_C 78.6), demonstrating the formation of a macrocyclic ring with the tetradecanoyl residue (Figure 1). The anomeric configurations of monosaccharides were determined from the magnitude of the $J_{1,2}$ coupling constants observed in the 1H NMR spectrum (Table 1). The doublet signals at δ_H 4.71 (Fuc H-1, $J = 7.8$ Hz) and δ_H 5.76 (Glc H-1, $J = 7.8$ Hz) indicated β -configurations for the fucose and glucose units, respectively. While the broad singlet signals at δ_H 5.68 (Rha H-1) and δ_H 5.40 (Rha' H-1) suggested α -configurations for the rhamnose units, which was further supported by the characteristic chemical shift observed at the C-5 positions (Table 2).^{19–21} The absolute configuration of monosaccharide including D-Glc, D-Fuc, and L-Rha were established after acidic hydrolysis, chemical derivatization, and UPLC-HRMS analysis (Figure S103).

To determine the absolute configuration at the aglycone's chiral center (δ_H 3.86, Agly H-11), Mosher's method was employed. After acidic hydrolysis of the resin glycoside fraction (Fr.F), purified 11-hydroxytetradecanoic acid was separately esterified with S-(+)-MTPA-Cl and R-(−)-MTPA-Cl. Subsequent 1H NMR (400 MHz) analysis revealed a $\Delta\delta$ ($\delta_{S\text{-ester}} - \delta_{R\text{-ester}}$) value of -0.07 ppm (-27.4 Hz) for the methyl protons, indicating that the C-11 center has the S-configuration (Figures S94 and S95), consistent with reported data for 11S-convolvulinolic acid in the literature.²² Consequently, the structure of compound 1 was established as (11S)-convolvulinolic acid 11-O- α -L-rhamnopyranosyl-(1 \rightarrow 3)-O-(4-O-isobutyryl)- α -L-rhamnopyranosyl-(1 \rightarrow 2)-O-(6-O-acetyl)- β -D-glucopyranosyl-(1 \rightarrow 2)-O- β -D-fucopyranoside, intramolecular 1,2''-ester and named campestridin A.

Compound 2 was isolated as a white amorphous powder, and its HRESIMS data (m/z 939.4795 [$M + H$]⁺, calcd. 939.4795) established the molecular formula as $C_{44}H_{74}O_{21}$. The 1H NMR spectrum revealed an isobutyryl group [δ_H 2.50 (Iba H-2, h, $J = 7.0$ Hz), 1.11 (Iba H-3, d, $J = 7.0$ Hz), 1.11 (Iba H-4, d, $J = 7.0$ Hz)] and an acetyl group at δ_H 1.82 (Ac H-2, s) (Table 1). Based on the mass difference ($\Delta m/z$ 28) compared to compound 1, it was inferred that one of the acetyl groups in Compound 1 was replaced by an isobutyryl group in compound 2. By examination of HMBC correlations from Glc H-6 (δ_H 4.55) to Ac C-1 (δ_C 170.8) and from Rha H-4 (δ_H 5.70) to Iba C-1 (δ_C 176.3), the positions of the acetyl and isobutyryl groups were confirmed (Figure 1). The absolute configurations of the monosaccharide units were determined in the same manner as for compound 1. On the basis of these results, compound 2 was identified as (11S)-convolvulinolic acid 11-O- α -L-rhamnopyranosyl-(1 \rightarrow 3)-O-(4-O-isobutyryl)- α -L-rhamnopyranosyl-(1 \rightarrow 2)-O-(6-O-acetyl)- β -D-glucopyranosyl-(1 \rightarrow 2)-O- β -D-fucopyranoside, intramolecular 1,2''-ester and named campestridin B.

Compound 3 was purified as a white amorphous powder, and its molecular formula was determined to be $C_{44}H_{76}O_{20}$ based on HRESIMS data (m/z 925.5004 [$M + H$]⁺, calcd. 925.5002). Its 1D NMR spectra closely resembled those of compound 1. However, the key difference is that the 1H NMR data of compound 3 displayed a methyl signal corresponding to a hexanoyl moiety [δ_H 0.77 (Hexa H-6, t, $J = 7.0$ Hz)], in contrast to the two methyl signals attributed to the two acetyl groups in compound 1 (Table 1). HMBC analysis was insufficient to

determine the linkage sites of the hexanoyl group and the aglycone on the Rha moiety due to the overlapped signals at δ_C 173.2 (Hexa C-1 and Agly C-1) in the ^{13}C NMR spectrum. Therefore, the exact position of the hexanoyl group at Rha C-4 was further confirmed by a ROESY correlation between Rha H₃-6 (δ_H 1.67) and Hexa H₂-2 (δ_H 2.27) (Figures 1 and S39). The absolute configurations of the monosaccharides and aglycone were established by using the same protocols applied for compound 1. These combined data supported the structural assignment of compound 3 as (11*S*)-convolvulinolic acid 11-O- α -L-rhamnopyranosyl-(1 \rightarrow 3)-O-(4-O-hexanoyl)- α -L-rhamnopyranosyl-(1 \rightarrow 2)-O- β -D-glucopyranosyl-(1 \rightarrow 2)-O- β -D-fucopyranoside, intramolecular 1,2'''-ester and named as campestridin C.

Compound 4 was isolated as a white, amorphous powder. Molecular formula of compound 4 was determined as C₄₂H₇₂O₂₀ from HRESIMS data (*m/z* 897.4687 [M + H]⁺; calcd. 897.4690). The ^1H NMR spectrum of compound 4 closely resembled that of compound 2, except for the absence of the signal assignable to the acetyl group. The presence of the isobutyryl group was supported by the signals at δ_H 2.51 (Iba H-2, *h*, *J* = 7.0 Hz), δ_H 1.12 (Iba H-3, *d*, *J* = 7.0 Hz), and δ_H 1.11 (Iba H-4, *d*, *J* = 7.0 Hz) (Table 1). The location of the isobutyryl substituent was established through an HMBC correlation from Rha H-4 (δ_H 5.70) to Iba C-1 (δ_C 176.4) (Figure 1). After acid hydrolysis and derivatization as performed for compound 1, the absolute configurations of the sugars and aglycon's C-11 position were determined. Based on these results, the structure of compound 4 was elucidated as (11*S*)-convolvulinolic acid 11-O- α -L-rhamnopyranosyl-(1 \rightarrow 3)-O-(4-O-isobutyryl)- α -L-rhamnopyranosyl-(1 \rightarrow 2)-O- β -D-glucopyranosyl-(1 \rightarrow 2)-O- β -D-fucopyranoside, intramolecular 1,2'''-ester and named campestridin D.

Compound 5 was obtained as a white, amorphous powder. HRESIMS data (*m/z* 927.4794 [M + H]⁺; calcd. 927.4795) established its molecular formula as C₄₃H₇₄O₂₁. The ^1H NMR spectrum was highly similar to that of compound 4. The key difference between compounds 4 and 5 was the replacement of the isobutyryl group in compound 4 with a niloyl group in compound 5, as suggested by the presence of two methyl signals [δ_H 1.20 (Nla H-5, *d*, *J* = 7.2 Hz), 1.28 (Nla H-4, *d*, *J* = 6.2 Hz)] and an oxygenated methine proton [δ_H 4.23 (Nla H-3, *m*)] (Table 3). This assumption was further supported by the COSY correlations of Nla H-3/H-4/H-5 as well as by the mass difference ($\Delta m/z$ 30) relative to that of the isobutyryl group in compound 4 (Figure 2). The position of the niloyl group was established by an HMBC correlation from Rha H-4 (δ_H 5.82) to Nla C-1 (δ_C 175.5) (Figure 2). The absolute configuration of the niloyl group was determined through alkaline hydrolysis of resin glycoside fraction (Fr.F), followed by comparison of the 1D NMR data and the specific rotation value of the resulting 4-bromophenacyl nitrate. Consequently, the structure of compound 5 was determined to be (11*S*)-convolvulinolic acid 11-O- α -L-rhamnopyranosyl-(1 \rightarrow 3)-O-[4-O-(2*R*,3*R*)-niloyl]- α -L-rhamnopyranosyl-(1 \rightarrow 2)-O- β -D-glucopyranosyl-(1 \rightarrow 2)-O- β -D-fucopyranoside, intramolecular 1,2'''-ester and named as campestridin E.

Compound 6 was isolated as a white amorphous powder, and its HRESIMS data (*m/z* 971.5049 [M + H]⁺, calcd. 971.5057) established the molecular formula as C₄₅H₇₈O₂₂. In the ^1H NMR spectrum, the presence of one isobutyryl group [δ_H 2.64 (Iba H-2, *h*, *J* = 7.0 Hz), 1.19 (Iba H-3, *d*, *J* = 7.0 Hz), 1.19 (Iba H-4, *d*, *J* = 7.0 Hz)] and an acetyl group [δ_H 1.95 (Ac H-2, *s*)] was

Table 3. ^1H NMR Spectroscopic Data for Compounds 5–7 in Pyridine-*d*₅

Position	5 ^a	6 ^b	7 ^b
Fuc-1	4.71, d (7.8)	4.76, d (7.7)	-
2	4.76, dd (7.8, 9.2)	4.50, dd (7.7, 9.2)	-
3	4.23, m	4.36, m	-
4	3.92, br s	4.09, br s	-
5	3.75, q (6.3)	3.90, m	-
6	1.50, d (6.3)	1.58, d (6.5)	-
Qui-1	-	-	4.80, d (7.8)
2	-	-	4.53, m
3	-	-	4.29, m
4	-	-	3.57, dd (8.6, 8.6)
5	-	-	3.66, dq (6.1, 8.6)
6	-	-	1.56, d (6.1)
Glc-1	5.83, d (7.7)	5.53, d (7.7)	6.02, d (7.4)
2	3.94, dd (7.7, 8.6)	4.20, dd (7.7, 9.2)	3.97, dd (7.4, 8.6)
3	4.12, m	4.13, br t (9.2)	4.16, m
4	4.08, m	3.97, br t (9.2)	4.06, m
5	3.57, dt (4.1, 9.2)	3.63, m	3.86, m
6a	4.08, m	4.69, m	4.21, m
6b	4.08, m	4.69, m	4.36, m
Rha-1	5.73, br s	6.36, br s	5.76, br s
2	6.16, br s	4.97, br s	6.12, br s
3	4.78, dd (3.3, 9.8)	5.02, dd (3.2, 9.9)	4.71, dd (3.2, 9.7)
4	5.82, t (9.8)	5.99, t (9.9)	5.74, t (9.7)
5	4.98, m	5.20, dq (6.2, 9.9)	4.97, m
6	1.75, d (6.2)	1.59, d (6.2)	1.71, d (6.3)
Rha'-1	5.46, br s	5.69, br s	5.45, br s
2	4.58, br s	4.58, br s	4.55, br s
3	4.53, dd (3.1, 9.4)	4.54, dd (3.4, 9.3)	4.51, m
4	4.26, br t (9.4)	4.24, t (9.3)	4.26, m
5	4.40, dq (6.2, 9.4)	4.69, m	4.38, m
6	1.62, d (6.2)	1.52, d (6.2)	1.62, d (6.2)
Agly-2a	2.21, ddd (3.6, 9.4, 13.8)	2.34, t (7.4)	2.20, m
2b	2.31, ddd (3.6, 8.1, 13.8)	-	2.30, m
3a	1.49, m	1.63, m	1.48, m
3b	1.62, m	-	1.61, m
4a	1.26, m	1.30, m	1.26, m
4b	1.40, m	-	1.40, m
11	3.85, m	3.90, m	3.86, m
12a	1.50, m	1.64, m	1.51, m
12b	1.70, m	1.80, m	1.73, m
13	1.48, m	1.58, m	1.51, m
14	0.85, t (7.2)	0.94, t (7.3)	0.87, t (7.0)
Nla-2	2.66, p (7.2)	-	2.50, p (7.2)
3	4.23, m	-	4.16, m
4	1.28, d (6.2)	-	1.29, d (6.2)
5	1.20, d (7.2)	-	1.13, d (7.2)
Iba-2	-	2.64, h (7.0)	-
3	-	1.19, d (7.0)	-
4	-	1.19, d (7.0)	-
Ac-2	-	1.95, s	-
OCH ₃	-	3.63, s	-

^aRecorded at 800 MHz. ^bRecorded at 900 MHz.

confirmed (Table 3). Additionally, the positions of the acetyl and isobutyryl groups were determined through HMBC correlations from Glc H-6 (δ_H 4.69) to Ac C-1 (δ_C 170.8) and from Rha H-4 (δ_H 5.99) to Iba C-1 (δ_C 176.1), respectively (Figure 2). In compound 6, the ^1H NMR spectrum showed a

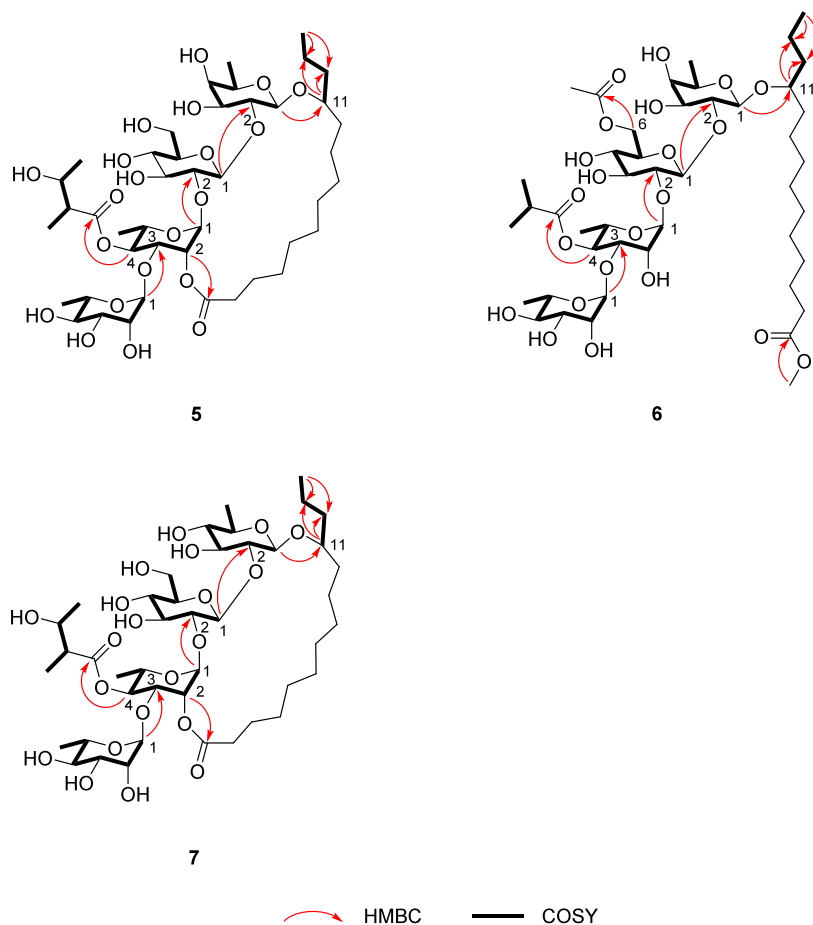


Figure 2. Key HMBC and COSY correlations of compounds 5–7.

merged signal for the methylene protons at δ_H 2.34 (Agly H-2, $J = 7.4$ Hz), in contrast to the diastereotopic Agly H-2 signals observed in compounds 1–5 and 7, suggesting that compound 6 likely has a nonmacrolactone structure. This assumption was further supported by the absence of an HMBC correlation between the oligosaccharide and aglycone via an ester linkage, whereas a clear HMBC correlation from Fuc H-1 ($\delta_H = 4.76$) to Agly C-11 ($\delta_C = 79.8$) was observed. The structure of the aglycone was determined to be 11-hydroxytetradecanoic acid methyl ester based on the COSY correlations of H₃-14/H₂-13/H₂-12/H₁-11, along with the HMBC correlation from OCH₃ (δ_H 3.63) to Agly C-1 (δ_C 174.0) (Figure 2). The absolute configurations of the monosaccharide units were determined as in compound 1, and the S configuration at aglycone C-11 was confirmed by Mosher's method. Based on these results, the structure of compound 6 was elucidated as (11S)-convolvulinolic acid 11-O- α -L-rhamnopyranosyl-(1→3)-O-[4-O-(2R,3R)-niloyl]- α -L-rhamnopyranosyl-(1→2)-O- β -D-glucopyranosyl-(1→2)-O- β -D-fucopyranoside methyl ester, named campestridin F.

Compound 7 was isolated as a white, amorphous powder. The molecular formula was determined to be C₄₃H₇₄O₂₁ based on HRESIMS data (m/z 927.4790 [M + H]⁺, calcd. 927.4795), which is identical with that of compound 5. Moreover, its ¹H and ¹³C NMR spectra closely resembled those of compound 5, except for the presence of quinovose in place of fucose (Tables 3 and 4).

The position of the niloyl and corresponding monosaccharide units were further confirmed through analysis of HSQC, HMBC, and COSY NMR data (Figure 2). The presence of

quinovose was determined by a proton signal at δ_H 3.57 (Qui H-3, dd, $J = 8.6, 8.6$ Hz) and its coupling constants (J), which was further confirmed by comparison with authentic standards in the LC-MS analysis after acid hydrolysis and subsequent derivatization (Figure S103). Consequently, the structure of compound 7 was established as (11S)-convolvulinolic acid 11-O- α -L-rhamnopyranosyl-(1→3)-O-[4-O-(2R,3R)-niloyl]- α -L-rhamnopyranosyl-(1→2)-O- β -D-glucopyranosyl-(1→2)-O- β -D-quino-pyranoside, intramolecular 1,2"-ester and named as campestridin G.

All isolated compounds (1–7) were assessed for their inhibitory activity against NO production in LPS-induced RAW 264.7 cells. None of the compounds were cytotoxic to RAW264.7 cells at their effective concentrations. Compounds 2 and 3 exhibited significant inhibitory effects with IC₅₀ values of 14.3 and 10.4 μ M, respectively (the IC₅₀ value of amino-guanidine as a positive control was 17.2 μ M) (Table 5). The structure–activity relationship of compounds isolated from *C. campestris* was analyzed based on their inhibition of nitric oxide production. Compound 6, which lacks the macrocyclic bridge between the aglycone and Rha compared to compound 2, exhibited reduced activity, highlighting the structural importance of this linkage. Furthermore, among compounds 3–5, the presence of an n-hexanoyl substituent at the C-4 position of rhamnose in compound 3 conferred the strongest inhibitory activity (IC₅₀ = 10.4 μ M). These findings suggest that variations in lipophilicity, driven by carbon chain substitutions, play a key role in modulating the inhibitory effects of these compounds.

Table 4. ^{13}C NMR Spectroscopic Data for Compounds 5–7 in Pyridine- d_5

Position	5^a	6^b	7^b
	δ_{C} , type	δ_{C} , type	δ_{C} , type
Fuc-1	102.2, CH	102.4, CH	-
2	74.8, CH	78.7, CH	-
3	76.6, CH	76.5, CH	-
4	73.3, CH	73.2, CH	-
5	71.2, CH	71.2, CH	-
6	17.3, CH_3	17.4, CH_3	-
Qui-1	-	-	101.9, CH
2	-	-	76.8, CH
3	-	-	79.3, CH
4	-	-	77.3, CH
5	-	-	72.6, CH
6	-	-	18.6, CH_3
Glc-1	100.7, CH	102.4, CH	100.5, CH
2	84.9, CH	77.9, CH	84.6, CH
3	77.8, CH	79.0, CH	78.0, CH
4	72.4, CH	71.6, CH	72.5, CH
5	77.0, CH	74.5, CH	77.7, CH
6	62.5, CH_2	64.6, CH_2	62.9, CH_2
Rha-1	100.1, CH	101.8, CH	99.8, CH
2	72.9, CH	71.9, CH	72.9, CH
3	76.2, CH	78.7, CH	75.9, CH
4	73.7, CH	74.1, CH	73.9, CH
5	67.2, CH	67.1, CH	67.0, CH
6	18.9, CH_3	18.3, CH_3	19.0, CH_3
Rha'-1	104.0, CH	104.4, CH	103.9, CH
2	72.5, CH	72.7, CH	72.5, CH
3	72.6, CH	72.6, CH	72.6, CH
4	73.9, CH	74.0, CH	73.9, CH
5	70.7, CH	70.1, CH	70.7, CH
6	18.6, CH_3	18.6, CH_3	18.6, CH_3
Agly-1	173.2, C	174.0, C	173.2, C
2	35.0, CH_2	34.2, CH_2	35.0, CH_2
3	26.1, CH_2	25.3, CH_2	26.2, CH_2
4	28.3, CH_2	29.5, CH_2	28.3, CH_2
11	78.9, CH	79.8, CH	79.0, CH
12	37.8, CH_2	37.6, CH_2	37.8, CH_2
13	19.2, CH_2	18.9, CH_2	19.2, CH_2
14	14.4, CH_3	14.5, CH_3	14.3, CH_3
Nla-1	175.5, C	-	175.5, C
2	48.7, CH	-	48.7, CH
3	69.3, CH	-	69.5, CH
4	21.4, CH_3	-	21.4, CH_3
5	14.2, CH_3	-	14.1, CH_3
Iba-1	-	176.1, C	-
2	-	34.7, CH	-
3	-	19.2, CH_3	-
4	-	19.2, CH_3	-
Ac-1	-	170.8, C	-
2	-	20.8, CH_3	-
OCH ₃	-	51.3, CH_3	-

^aRecorded at 200 MHz. ^bRecorded at 225 MHz.

CONCLUSION

In conclusion, seven previously undescribed resin glycosides (Campestridin A–G) were isolated and characterized from *C. campestris*, guided by LC-HRMS/MS-based molecular networking. Structural elucidation using 1D and 2D NMR, combined with HRESIMS, revealed that these compounds

Table 5. Inhibitory Effects of Compounds 1–7 on NO Production in LPS-Induced RAW 264.7 Cells

Compounds	(μM) ^a	Compounds	(μM) ^a
1	35.4 ± 0.8	5	>50
2	14.3 ± 0.7	6	31.7 ± 2.4
3	10.4 ± 0.2	7	>50
4	23.4 ± 2.8	PC ^b	17.2 ± 0.5

^aResults were indicated as the mean IC_{50} ± SD values in μM from triplicated experiments. ^bPositive control: aminoguanidine.

possess tetrasaccharide moieties consisting of D-glucose, D-fucose, D-quinovose, and L-rhamnose, each bearing various acyl modifications. These oligosaccharide cores match those of the previously reported tricolorins A–E, which are the major resin glycosides of *Ipomoea tricolor*.²³ The absolute configurations of their aglycones were determined by Mosher's method following acid hydrolysis. The bioactivity evaluation demonstrated that among the isolates, compounds 2 and 3 significantly inhibited NO production in LPS-induced RAW 264.7 cells, with IC_{50} values of 14.3 and 10.4 μM , respectively. Structure–activity relationship analysis suggested that the presence of acyl groups, such as an *n*-hexanoyl group at the C-4 position of rhamnose, may enhance the inhibitory activity. These findings highlight the bioactive potential of resin glycosides of *C. campestris* and support the continued investigation of natural products within the Convolvulaceae family.

Overall, this study demonstrated the effectiveness of LC-MS-based molecular networking as a targeted strategy for the discovery of novel natural products with promising bioactivity. Further studies, including mechanistic and *in vivo* evaluations, are needed to assess the therapeutic potential of these newly identified compounds in inflammatory-related disorders.

EXPERIMENTAL SECTION

General Experimental Procedures. Optical rotations and UV spectra were recorded using a JASCO DIP-1000 polarimeter and JASCO UV-550 spectrophotometer (JASCO, Tokyo, Japan), respectively. 1D and 2D NMR spectra were recorded using Bruker AVANCE 400, 800, and 900 MHz spectrometers (Bruker, MA, USA). HRESIMS and LC-HRMS/MS analyses were performed by using an Orbitrap Exploris 120 mass spectrometer coupled with a Vanquish UHPLC system and a diode array detector (Thermo Fisher Scientific, MA, USA). MPLC was performed using a Biotage Isolera Prime chromatography system and a Selekt Flash Purification System. Semipreparative HPLC was performed on a Waters HPLC system equipped with two Waters S15 pumps and a 2996 photodiode-array detector using YMC J'sphere ODS-H80 (4 μm , 250 × 20 mm, i.d., flow rate 10 mL/min) and J'sphere ODS-H80 (4 μm , 150 × 20 mm, i.d., flow rate 6 mL/min). TLC was performed on precoated silica gel 60 F₂₅₄ (0.25 mm, Merck) plates, and spots were visualized using a 10% vanillin-H₂SO₄/water spray reagent.

Plant Materials. The whole plants of *Cuscuta campestris* (Convolvulaceae) were collected in Yeongdong-gun, Chungcheongbuk-do, Republic of Korea in October 2023, and authenticated by Prof. Bang Yeon Hwang. The voucher specimen has been deposited at the Herbarium of the College of Pharmacy, Chungbuk National University, Republic of Korea.

Extraction and Isolation. Whole plants of dried *C. campestris* (1.0 kg) were extracted with MeOH (2 × 10 L) by maceration for 3 days at room temperature to obtain the MeOH extracts (56.0 g). The MeOH extracts was resuspended in water and successively partitioned with *n*-hexane (2 × 1 L), dichloromethane (2 × 1 L), and EtOAc (2 × 1 L).

The EtOAc-soluble fraction (3.9 g) was subjected to RP MPLC using a MeOH-H₂O step gradient system (10:90 to 100:0) to obtain nine subfractions (Fr.A–Fr.I). Fr.F (583.5 mg) was further separated

using Sephadex LH-20 open column chromatography with 100% MeOH to yield six subfractions (Fr.F.1–Fr.F.6). Fr.F.4 (100.3 mg) was separated by RP MPLC using a MeOH-H₂O step gradient system (60:40 to 100:0), resulting in eight subfractions (Fr.F.4.A–Fr.F.4.H). Fr.F.4.C (52.9 mg) was subjected to preparative HPLC with a CH₃CN-H₂O isocratic elution system (50:50 to 100:0, flow rate of 10.0 mL/min) to isolate compounds 5 (2.3 mg) and 7 (4.7 mg). Fr.F.4.D (28.8 mg) was separated by preparative HPLC (CH₃CN-H₂O, 55:45 to 100:0, flow rate 10.0 mL/min) to obtain compound 6 (1.8 mg). Fr.F.4.F (29.0 mg) was processed by preparative HPLC (CH₃CN-H₂O, 60:40 to 100:0, flow rate 10.0 mL/min) to isolate compound 4 (1.8 mg). Fr.F.4.H (16.5 mg) was subjected to preparative HPLC (CH₃CN-H₂O, 60:40 to 100:0, flow rate of 10.0 mL/min) to obtain compound 3 (1.1 mg). Fr.F.5 (142.4 mg) was also separated by preparative HPLC (CH₃CN-H₂O, 60:40 to 100:0, flow rate 10.0 mL/min) to isolate compounds 1 (1.1 mg) and 2 (3.4 mg). The purity of each compound was confirmed by using TLC.

Campestridin A (1). White amorphous powder; $[\alpha]_D^{25} -22.6$ (*c* 0.6, MeOH); ¹H NMR (900 MHz, pyridine-*d*₅) and ¹³C NMR (225 MHz, pyridine-*d*₅), see Tables 1 and 2, respectively; HRESIMS *m/z* 911.4483 [M + H]⁺ (calcd for C₄₂H₇₁O₂₁⁺, 911.4482).

Campestridin B (2). White amorphous powder; $[\alpha]_D^{25} -86.0$ (*c* 2.9, MeOH); ¹H NMR (400 MHz, pyridine-*d*₅) and ¹³C NMR (100 MHz, pyridine-*d*₅), see Tables 1 and 2, respectively; HRESIMS *m/z* 939.4795 [M + H]⁺ (calcd for C₄₄H₇₅O₂₁⁺, 939.4795).

Campestridin C (3). White amorphous powder; $[\alpha]_D^{25} -31.7$ (*c* 0.6, MeOH); ¹H NMR (900 MHz, pyridine-*d*₅) and ¹³C NMR (225 MHz, pyridine-*d*₅), see Tables 1 and 2, respectively; HRESIMS *m/z* 925.5004 [M + H]⁺ (calcd for C₄₄H₇₇O₂₀⁺, 925.5002).

Campestridin D (4). White amorphous powder; $[\alpha]_D^{25} -37.2$ (*c* 1.3, MeOH); ¹H NMR (900 MHz, pyridine-*d*₅) and ¹³C NMR (225 MHz, pyridine-*d*₅), see Tables 1 and 2, respectively; HRESIMS *m/z* 897.4687 [M + H]⁺ (calcd for C₄₂H₇₃O₂₀⁺, 897.4690).

Campestridin E (5). White amorphous powder; $[\alpha]_D^{25} -40.2$ (*c* 1.8, MeOH); ¹H NMR (800 MHz, pyridine-*d*₅) and ¹³C NMR (200 MHz, pyridine-*d*₅), see Tables 3 and 4, respectively; HRESIMS *m/z* 927.4794 [M + H]⁺ (calcd for C₄₃H₇₅O₂₁⁺, 927.4795).

Campestridin F (6). White amorphous powder; $[\alpha]_D^{25} -90.8$ (*c* 1.3, MeOH); ¹H NMR (900 MHz, pyridine-*d*₅) and ¹³C NMR (225 MHz, pyridine-*d*₅), see Tables 3 and 4, respectively; HRESIMS *m/z* 971.5049 [M + H]⁺ (calcd for C₄₅H₇₉O₂₂⁺, 971.5057).

Campestridin G (7). White amorphous powder; $[\alpha]_D^{25} -46.7$ (*c* 2.1, MeOH); ¹H NMR (900 MHz, pyridine-*d*₅) and ¹³C NMR (225 MHz, pyridine-*d*₅), see Tables 3 and 4, respectively; HRESIMS *m/z* 927.4790 [M + H]⁺ (calcd for C₄₃H₇₅O₂₁⁺, 927.4795).

UHPLC-HRMS/MS Analysis and Molecular Networking. UHPLC-HRMS/MS analysis was carried out using an Orbitrap Exploris 120 mass spectrometer integrated with a Vanquish UHPLC system and a diode array detector. The *n*-hexane, dichloromethane, and EtOAc-soluble fractions were analyzed via LC-MS/MS using a YMC-Triart C18 column (100 × 2.1 mm, 1.9 μm). A gradient elution system was employed, transitioning from 90:10 (A:B) to 0:100 over 11 min at a flow rate of 0.3 mL/min. The mobile phase consisted of H₂O (A) and CH₃CN (B), both containing 0.1% formic acid. The sample injection volume was maintained at 2 μL, while the column temperature was set to 30 °C. Mass detection was conducted within an *m/z* range of 100–2000, with the Orbitrap analyzer operating at a resolution of 60,000 for full MS scans and 15,000 for data-dependent MS_n scans. The HESI source parameters were configured as follows: spray voltage of 3.5 kV, vaporizer temperature of 275 °C, ion transfer tube temperature of 320 °C, sheath gas flow rate of 50 L/min, auxiliary gas flow rate of 15 L/min, and sweep gas flow rate of 1 L/min. Ion fragmentation was performed using a normalized HCD energy of 30%. To ensure efficient spectral acquisition, the data-dependent MS_n mode was applied, capturing the MS₂ spectra for the four most abundant ions. A dynamic exclusion window of 2.5 s was implemented to prevent redundant ion fragmentation. The LC-HRMS/MS raw data were first converted into an mzXML format using MSConvert software, followed by data processing in MZmine 4.2. Spectral clustering and molecular networking were conducted through the Global Natural Products

Social Molecular Networking (GNPS) platform, utilizing an analytical workflow with a cosine similarity threshold of 0.7 and a minimum requirement of five matched peaks for clustering. The generated molecular networks were subsequently visualized by using Cytoscape software (version 3.10.0).

Sugar Analysis. A mixture of compounds 1–6 (0.05 mg each) and compound 7 (0.3 mg) were hydrolyzed in 1 mL of 3 N HCl under reflux at 90 °C for 2 h. The reaction mixtures were then concentrated *in vacuo* to obtain the sugar fraction. The hydrolysates were dissolved in 1 mL of anhydrous pyridine along with L-cysteine methyl ester hydrochloride (1 mg) and incubated at 60 °C for 1 h. Afterward, 10 μL of phenyl isothiocyanate was added, and the reaction was further incubated at 60 °C for 1 h.^{24–26} The derivatized sugar samples were analyzed by using a UHPLC-HRESIMS system. The separation was performed on a YMC-Triart C₁₈ column (100 × 2.1 mm, 1.9 μm) at 30 °C. The mobile phase consisted of H₂O (A) and CH₃CN (B), both containing 0.1% formic acid, with a gradient elution system (A:B, 80:20 to 70:30 over 16 min). The flow rate was set to 0.3 mL/min, and the sample injection volume was 2 μL. The retention times of derivatized D-glucose (*t*_R 8.2 min, *m/z* 433.1096), D-fucose (*t*_R 10.4 min, *m/z* 417.1149), D-quinovose (*t*_R 11.4 min, *m/z* 417.1147), and L-rhamnose (*t*_R 12.3 min, *m/z* 417.1147) were determined using authenticated standards (Figure S103), which were subjected to the same derivatization and UHPLC-MS analysis conditions as the samples for accurate comparison.

Identification of Aglycones. The resin glycoside fraction (Fr.F, 60.0 mg) was hydrolyzed in 10 mL of 3 N HCl under reflux at 90 °C for 2 h. The hydrolysate was cooled to room temperature and extracted with EtOAc (10 mL × 2) to obtain a mixture of aglycones (17.3 mg). The organic layer was then subjected to prep-HPLC (J'sphere ODS-H80, 4 μm, 250 × 20 mm, i.d., flow rate 10 mL/min) using a gradient elution of H₂O:CH₃CN (70:30 to 0:100) to yield 11-hydroxytetradecanoic acid (4.3 mg) and 11-hydroxytetradecanoic acid methyl ester (1.5 mg) (Figure S89). A 4 mL vial containing obtained hydroxy fatty acids (0.1 mg each) and anhydrous pyridine (1 μL) in 100 μL of CDCl₃ was treated with (S)-(+)-α-methoxy-α-trifluoromethylphenylacetyl chloride (S(+)-MTPA-Cl, 2 μL) at room temperature for 2 h. The reaction with R(-)-MTPA-Cl was conducted identically. Subsequent ¹H NMR (400 MHz) analysis of the resulting Mosher esters revealed a Δδ (δ_S -ester – δ_R -ester) value of –0.07 ppm (–27.4 Hz) for the methyl protons, indicating that the C-11 center of both 11-hydroxytetradecanoic acid and 11-hydroxytetradecanoic acid methyl ester has the S-configuration.²²

(S)-11-Hydroxytetradecanoic Acid (8). Colorless oil; ¹H NMR (400 MHz, Pyridine-*d*₅) δ_H 3.84 (1H, m, H-11), 2.53 (2H, t, *J* = 7.4 Hz, H-2), 0.97 (3H, t, *J* = 7.0 Hz, H-14); ¹³C NMR (100 MHz, Pyridine-*d*₅) δ_C 175.1, 70.6, 40.7, 38.6, 35.0, 30.2, 30.0, 29.8, 29.7, 29.6, 26.4, 25.7, 19.5, 14.6; HRESIMS *m/z* 267.1931 [M + Na]⁺ (Calcd for C₁₄H₂₈O₃Na⁺ 267.1931), see Figures S90 and S91.

(S)-11-Hydroxytetradecanoic Acid Methyl Ester (9). Colorless oil; ¹H NMR (400 MHz, Pyridine-*d*₅) δ_H 3.84 (1H, m, H-11), 3.64 (3H, s, OCH₃), 2.33 (2H, t, *J* = 7.4 Hz, H-2), 0.97 (3H, t, *J* = 7.0 Hz, H-14); ¹³C NMR (100 MHz, Pyridine-*d*₅) δ_C 173.9, 70.6, 51.3, 40.7, 38.6, 34.1, 30.2, 30.0, 29.7, 29.6, 29.4, 26.4, 25.3, 19.5, 14.6; HRESIMS *m/z* 281.2087 [M + Na]⁺ (Calcd for C₁₅H₃₀O₃Na⁺ 281.2087), see Figures S92 and S93.

Identification of Nilic Acid. The resin glycoside fraction (Fr.F, 60.0 mg) was hydrolyzed in 10 mL of 5% KOH under reflux at 95 °C for 3 h. The reaction mixture was acidified to pH 4.0 with 1 N HCl and extracted with EtOAc (10 mL × 2) to obtain a mixture of organic acids (10.5 mg). The organic layer evaporated and treated with triethylamine (20 μL) and 4-bromophenacyl bromide (10 mg) in dried acetone (5 mL) at room temperature for 2 h. The reaction mixture was concentrated, diluted with H₂O (5 mL), and extracted with Et₂O (5 mL × 2). The resulting residue was subjected to prep-HPLC (J'sphere ODS-H80, 4 μm, 150 × 20 mm, i.d., flow rate 6 mL/min) with an isocratic elution of H₂O:CH₃CN (50:50) to give a 4-bromophenacyl nitrate (*t*_R 17 min, 1.1 mg). The configuration of nilic acid was determined as (2*R*,3*R*) by comparing the 1D NMR spectra and the specific rotation value of the 4-bromophenacyl ester with data reported in the literature.^{27,28}

4-Bromophenacyl-(2R,3R)-nilate (14). White amorphous powder; $[\alpha]_D^{25} -7.5$ (*c* 0.1, CHCl_3); ^1H NMR (400 MHz, CDCl_3) δ H 7.78 (2H, br d, *J* = 8.5 Hz), 7.65 (2H, br d, *J* = 8.5 Hz), 5.33 (1H, d, *J* = 16.6 Hz), 5.44 (1H, d, *J* = 16.6 Hz), 3.97 (1H, m, H-3), 2.62 (1H, m, H-2), 1.30 (3H, d, *J* = 6.3 Hz, H-4), 1.25 (3H, d, *J* = 7.0 Hz, H-5), see Figures S101 and S102; HRESIMS *m/z* 337.0046 [M + Na]⁺ (Calcd for $C_{13}\text{H}_{15}\text{BrO}_4\text{Na}^+$ 337.0051).

Inhibition of Nitric Oxide Production and Cell Toxicity. RAW 264.7 cells, originally sourced from the American Type Culture Collection (ATCC, Manassas, VA, USA), were maintained in Dulbecco's Modified Eagle's Medium (DMEM; Gibco-BRL, St. Louis, MO, USA) supplemented with 5% heat-inactivated fetal bovine serum, along with 100 U/mL penicillin and 100 $\mu\text{g}/\text{mL}$ streptomycin. The cultures were incubated under controlled conditions at 37 °C under a humidified atmosphere containing 5% CO_2 . Cells were seeded at a density of 2×10^5 cells per well in a 96-well plate and allowed to adhere for 6 h before treatment. The test compounds and extracts were initially dissolved in dimethyl sulfoxide (DMSO) and subsequently diluted in DMEM to obtain the required working concentrations: methanol extracts and fractions (0.4–10 $\mu\text{g}/\text{mL}$), aminoguanidine (0.5–10 μM), and isolated compounds (2–20 μM). To induce nitric oxide (NO) production, lipopolysaccharide (LPS) was introduced at a final concentration of 100 ng per well. After 24 h of incubation at 37 °C, nitrite accumulation in the culture supernatant was quantified using the Griess reaction. In this assay, 100 μL of the cell-free supernatant was mixed with 100 μL of Griess reagent, composed of 2% (w/v) sulfanilamide in 5% (w/v) phosphoric acid and 0.2% (w/v) *N*-(1-naphthyl) ethylenediamine dihydrochloride in equal proportions. The absorbance was measured at 550 nm, and the nitrite concentration was calculated using a standard curve generated with sodium nitrite solutions. To assess cell viability, the remaining adherent cells were subjected to the MTT assay using 3-(4,5-dimethylthiazol-2-yl)-2,5-diphenyltetrazolium bromide (MTT) reagent (Sigma Chemical Co., St. Louis, MO, USA), and absorbance was measured at 570 nm.

■ ASSOCIATED CONTENT

Data Availability Statement

The raw NMR data for campestridins A-G (1–7) have been deposited in the Natural Products Magnetic Resonance Database (NP-MRD; www.np-mrd.org) and can be found at NP0351463 (campestridin A), NP0351464 (campestridin B), NP0351465 (campestridin C), NP0351466 (campestridin D), NP0351467 (campestridin E), NP0351468 (campestridin F), and NP0351469 (campestridin G).

§ Supporting Information

The Supporting Information is available free of charge at <https://pubs.acs.org/doi/10.1021/acs.jnatprod.5c00713>.

Molecular networking analysis; 1D and 2D NMR, and HRESIMS data for compounds 1–14 ([PDF](#))

■ AUTHOR INFORMATION

Corresponding Author

Bang Yeon Hwang — College of Pharmacy, Chungbuk National University, Cheongju 28160, Republic of Korea; orcid.org/0000-0002-4148-6751; Email: byhwang@chungbuk.ac.kr

Authors

Jae Sang Han — College of Pharmacy, Chungbuk National University, Cheongju 28160, Republic of Korea

Jun Gu Kim — College of Pharmacy, Chungbuk National University, Cheongju 28160, Republic of Korea

Yong Beom Cho — College of Pharmacy, Chungbuk National University, Cheongju 28160, Republic of Korea

Joon Su Jang — College of Pharmacy, Chungbuk National University, Cheongju 28160, Republic of Korea

Vu Quan Dang — College of Pharmacy, Chungbuk National University, Cheongju 28160, Republic of Korea

Dongho Lee — Department of Plant Biotechnology, College of Life Sciences and Biotechnology, Korea University, Seoul 02841, Republic of Korea; orcid.org/0000-0003-4379-814X

Mi Kyeong Lee — College of Pharmacy, Chungbuk National University, Cheongju 28160, Republic of Korea; orcid.org/0000-0001-5814-2720

Jin Woo Lee — Department of AI Drug Discovery, Duksung Women's University, Seoul 01369, Republic of Korea; orcid.org/0000-0002-0573-0884

Complete contact information is available at:
<https://pubs.acs.org/doi/10.1021/acs.jnatprod.5c00713>

Author Contributions

B. Y. H. conceived and designed the experiments; J. S. H. and Y. B. C. isolated, identified, and purified the resin glycosides. J. S. J. and V. Q. D. evaluated the NO production inhibitory activity of the crude extracts and isolated compounds; J. G. K., D. L., M. K. L., and J. W. L. analyzed the NMR and MS data; and J. S. H. and B. Y. H. wrote the manuscript. All authors have read and approved the final version of this manuscript.

Notes

The authors declare no competing financial interest.

■ ACKNOWLEDGMENTS

This research was supported by the National Research Foundation of Korea (NRF) grant funded by the Korea government (MSIT) (RS-2024-00440614 and RS-2025-02273102).

■ REFERENCES

- (1) Jakovljević, V. D.; Vrvić, M. M.; Vrbničanin, S.; Sarić-Krsmanović, M. *Chem. Biodivers.* **2018**, *15*, No. e1800174.
- (2) Ahmad, A.; Tandon, S.; Xuan, T. D.; Nooreen, Z. *Biomed. Pharmacother.* **2017**, *92*, 772–795.
- (3) Lee, M.-S.; Chen, C.-J.; Wan, L.; Koizumi, A.; Chang, W.-T.; Yang, M.-J.; Lin, W.-H.; Tsai, F.-J.; Lin, M.-K. *Process Biochem.* **2011**, *46*, 2248–2254.
- (4) Agha, A. M.; Sattar, E. A.; Galal, A. *Phytother. Res.* **1996**, *10*, 117–120.
- (5) Selvi, E. K.; Turumtay, H.; Demir, A.; Turumtay, E. A. *Anal. Lett.* **2018**, *51*, 1464–1478.
- (6) Hřibová, P.; Žemlička, M.; Bartl, T.; Švajdlenka, E. *Chem. Listy* **2009**, *103*, 243–245.
- (7) Löffler, C.; Czygan, F.-C.; Proksch, P. *Biochem. Syst. Ecol.* **1997**, *25*, 297–303.
- (8) Pereda-Miranda, R.; Rosas-Ramírez, D.; Castañeda-Gómez, J. Resin glycosides from the morning glory family. In *Fortschritte der Chemie organischer Naturstoffe/Progress in the Chemistry of Organic Natural Products*; Kinghorn, A. D.; Falk, H.; Kobayashi, J., Eds.; Springer: Vienna, 2010; Vol. 92, pp 77–153.
- (9) Fan, B. Y.; Jiang, X.; Li, Y. X.; Wang, W. L.; Yang, M.; Li, J. L.; Wang, A. D.; Chen, G. T. *Med. Res. Rev.* **2022**, *42* (6), 2025–2066.
- (10) Lira-Ricárdez, J.; Pereda-Miranda, R. *Phytochem. Rev.* **2020**, *19* (5), 1211–1229.
- (11) Govindarajan, M. *Eur. J. Med. Chem.* **2018**, *143*, 1208–1253.
- (12) Cao, S.; Norris, A.; Wisse, J. H.; Miller, J. S.; Evans, R.; Kingston, D. G. *Nat. Prod. Res.* **2007**, *21* (10), 872–876.
- (13) Rosas-Ramírez, D.; Escandon-Rivera, S.; Pereda-Miranda, R. *Phytochemistry* **2018**, *148*, 39–47.
- (14) Ono, M.; Takigawa, A.; Muto, H.; Kabata, K.; Okawa, M.; Kinjo, J.; Yokomizo, K.; Yoshimitsu, H.; Nohara, T. *Chem. Pharm. Bull. (Tokyo)* **2015**, *63* (8), 641–648.

- (15) Ono, M.; Kanemaru, Y.; Yasuda, S.; Okawa, M.; Kinjo, J.; Miyashita, H.; Yokomizo, K.; Yoshimitsu, H.; Nohara, T. *Nat. Prod. Res.* **2017**, *31* (22), 2660–2664.
- (16) Leon-Rivera, I.; Villeda-Hernandez, J.; Campos-Pena, V.; Aguirre-Moreno, A.; Estrada-Soto, S.; Navarrete-Vazquez, G.; Rios, M. Y.; Aguilar-Guadarrama, B.; Castillo-Espana, P.; Rivera-Leyva, J. C. *Bioorg. Med. Chem. Lett.* **2014**, *24* (15), 3541–3545.
- (17) Wang, M.; Carver, J. J.; Phelan, V. V.; Sanchez, L. M.; Garg, N.; Peng, Y.; Nguyen, D. D.; Watrous, J.; Kapono, C. A.; Luzzatto-Knaan, T.; et al. *Nat. Biotechnol.* **2016**, *34* (8), 828–837.
- (18) da Silva, R. R.; Wang, M.; Nothias, L. F.; van der Hooft, J. J. J.; Caraballo-Rodriguez, A. M.; Fox, E.; Balunas, M. J.; Klassen, J. L.; Lopes, N. P.; Dorrestein, P. C. *PLoS Comput. Biol.* **2018**, *14* (4), No. e1006089.
- (19) Seo, S.; Tomita, Y.; Tori, K.; Yoshimura, Y. *J. Am. Chem. Soc.* **1978**, *100* (11), 3331–3339.
- (20) Xu, J.-Y.; He, Y.; Zhang, A.-W.; Lu, Y.; Chen, G.-T.; Yang, M.; Fan, B.-Y. *Nat. Prod. Res.* **2021**, *35* (21), 3766–3771.
- (21) Li, Y.-X.; He, X.-J.; Chen, Y.; Gu, J.-P.; Qi, T.-Z.; Gu, H.; Zhu, X.-Y.; Yang, M.; Gu, Y.-C.; Ling, B.; et al. *J. Nat. Prod.* **2025**, *88* (2), 415–426.
- (22) Ono, M. *J. Nat. Med.* **2017**, *71* (4), 591–604.
- (23) Bah, M.; Pereda-Miranda, R. *Tetrahedron* **1996**, *52* (41), 13063–13080.
- (24) Tanaka, T.; Nakashima, T.; Ueda, T.; Tomii, K.; Kouno, I. *Chem. Pharm. Bull.* **2007**, *55* (6), 899–901.
- (25) Kim, J. G.; Lee, J. W.; Le, T. P. L.; Han, J. S.; Cho, Y. B.; Kwon, H.; Lee, D.; Lee, M. K.; Hwang, B. Y. *J. Nat. Prod.* **2021**, *84* (3), 562–569.
- (26) Castañeda-Gómez, J. F.; Leitão, S. G.; Pereda-Miranda, R. *Phytochemistry* **2023**, *211*, 113689.
- (27) Fan, B. Y.; Luo, J. G.; Gu, Y. C.; Kong, L. Y. *Tetrahedron* **2014**, *70* (11), 2003–2014.
- (28) Cruz-Morales, S.; Castañeda-Gómez, J.; Figueroa-González, G.; Mendoza-García, A. D.; Lorence, A.; Pereda-Miranda, R. *J. Nat. Prod.* **2012**, *75* (9), 1603–1611.

CAS BIOFINDER DISCOVERY PLATFORM™

**PRECISION DATA
FOR FASTER
DRUG
DISCOVERY**

CAS BioFinder helps you identify targets, biomarkers, and pathways

Unlock insights

CAS A division of the American Chemical Society